

## An adaptive PC-Kriging method for time-variant structural reliability analysis

Indexed by:



Hang Nan<sup>a</sup>, Hongshuang Li<sup>a,\*</sup>, Zhuocheng Song<sup>a</sup>

<sup>a</sup>Nanjing University of Aeronautics and Astronautics, College of Aerospace Engineering, Nanjing, 210016, China


### Highlights

- A PCK method with adaptive strategy is proposed to estimate the time-variant reliability.
- The U- and H- learning functions are integrated to update the PCK models.
- The proposed method is efficient for time-variant reliability problems with implicit LSF.

### Abstract

The practical application of time-variant reliability analysis is limited by its computationally expensive models which describe the structural system behavior. This paper presents a new adaptive PC-Kriging (APCK) approach to accurately and efficiently assess the time-variant reliabilities. Time interval is firstly discretized with a series of time instants and then the stochastic process is reconstructed by standard normal random variables and deterministic function of time. PC-Kriging (PCK) models are built at each time instant to predict the instantaneous responses of performance function. To improve the accuracy and efficiency, a new update strategy based on the integration of U- and H- learning functions is developed to refine the PCK models of instantaneous responses. One or two best samples are identified by the proposed learning criterion for updating the PCK models. Finally, Monte Carlo simulation (MCS) is used to estimate the time-variant reliability based on the updated PCK models. Four examples are used to validate the accuracy and efficiency of the proposed method.

### Keywords

This is an open access article under the CC BY license (<https://creativecommons.org/licenses/by/4.0/>) 

time-variant, reliability analysis, instantaneous response, adaptive PC-Kriging, learning function.

## 1. Introduction

Structural performance fluctuates since the existence of various uncertainties in realistic engineering. Reliability, as a significant engineering requirement, aims at calculating the probability that a structure fulfills its intended function within a specified period of time and under specified conditions by considering the input randomness [41]. Many structural reliability methods were developed in the past decades. The most probable point (MPP)-based methods are one of the classic reliability analysis techniques, including the first order reliability method (FORM) [38, 39] and the second order reliability method (SORM) [2]. Except for the MPP-based methods, the moment-based methods [34] and the surrogate-based methods [16] are also utilized to evaluate the time-invariant reliability. In fact, the degradation of material properties, stochastic loadings, and etc. indicate that uncertainties have time-variant characteristics, which result in the decrease of reliability over time. For this case, time-invariant reliability methods are not applicable and extensive attention is concerned on the time-variant reliability analysis. The introduction of time factor greatly increase the computational cost and difficulty of time-variant reliability problem. It is a great challenge to obtain the time-variant reliability in an accurate and efficient way.

Outcrossing rate based method first developed by Rice [29] is one of the dominant approaches for time-variant reliability analysis. The core content of this type of methods is to approximate the failure rate by the outcrossing rate. Based on this theory, many improved methods were developed in the past decades. Kanjilal and Manohar [14] estimated the conditional probability with respect to the random system parameters based on the outcrossing rate, and then computed its expectation to obtain the time-variant reliability. Zhang et al. [43] combined the Gauss-Legendre quadrature and outcrossing rate to efficiently estimate the time-variant reliability. Breitung [3] derived the analytical expression of outcrossing rate for stationary Gaussian processes by asymptotic approximations for integrals. For nonstationary non-Gaussian performance functions, Cai et al. [4] proposed a new analytical formula to obtain the mean outcrossing rate by transforming the performance functions into a standard Gaussian process. Andrieu-Renaud et al. [1] developed the PHI2 method which applies FORM to the parallel system time-invariant reliability analysis to compute the outcrossing rate. The accuracy of the PHI2 method greatly depends on the time step size, thus Sudret [33] proposed the improved PHI2 method to reduce the impact of time step size. Ebrahimian et al. [7] developed a PHI2 based algorithm for evaluating the time-variant reliability of the passive heat removal system. Instead of using the

(\*) Corresponding author.

E-mail addresses: H. Nan (ORCID: 0000-0002-6683-6156): [hangnan@nuaa.edu.cn](mailto:hangnan@nuaa.edu.cn), H. Li (ORCID: 0000-0001-8106-5786): [hongshuangli@nuaa.edu.cn](mailto:hongshuangli@nuaa.edu.cn), Z. Song (ORCID: 0000-0002-7091-089X): [maxwellsong@nuaa.edu.cn](mailto:maxwellsong@nuaa.edu.cn)

outcrossing rate, Quezada del Villar et al. [28] estimated the distribution of the first passage time in the outcrossing events to obtain the time-variant reliability. All the above-mentioned outcrossing rate based methods may successfully obtain the time-variant reliability. However, most approaches in this category are based on linear approximation and may result in large error and limited their applications, which lead to the worse accuracy for nonlinear cases.

The extreme value based methods are another tools for time-variant reliability analysis, which employ the information of response extreme value of structural performance function during service time. Chen and Li [6] used the probability density evolution method (PDEM) to evaluate the probability distribution of extreme value for obtaining time-variant reliability. A sampling approach was combined with saddlepoint approximation to estimate the extreme value distribution for time-variant reliability problem with one input stochastic process [10]. Xu [37] derived the equivalent extreme value distribution of structural response based on the maximum entropy principle to assess the dynamic reliability of structural systems. In general, the extreme value of structural response is highly nonlinear, therefore it is difficult to obtain an accurate estimation for the tail of its probability distribution which is the key domain for reliability analysis. For this reason, constructing a surrogate model for the response extreme value is a promising approaches. Wang and Wang [36] developed a nested extreme value surface (NERS) method, which combines the efficient global optimization (EGO) [21] and Kriging to construct a nested time prediction model for converting time-variant reliability problem into a time-invariant one. Hu and Du [11] proposed a mixed EGO algorithm to improve the efficiency of building up surrogate model for the extreme response by sampling random variables and time simultaneously. The above-mentioned surrogate model methods with double-loop process has the drawback of low efficiency. Therefore, Hu and Mahadevan [12] developed a single-loop Kriging surrogate model approach based on the elimination of the optimization loop. Qian et al. [26, 27] provided a decoupling strategy to avoid the inner optimization loop in the double-loop procedure by establishing the kriging model of extreme value response. Hu et al. [9] focused on the concept of first failure instant to efficiently construct a single-loop Kriging model for time-variant reliability analysis.

Except for the aforementioned two categories of classic methods, some different approaches for time-variant reliability analysis are also reported. Composite limit state methods (CLS) [23] discretize the time interval of interest to obtain the instantaneous limit state function as the components of a series system, and then the time-variant reliability is assessed by time-invariant series system reliability methods. Li et al. [19] proposed an improved composite limit state method, Kriging models of all time nodes and one CLS are constructed to estimate the time-variant reliability. Zhang et al. [42] also inspired by the transformation of a time-variant reliability problem into time-invariant reliability problem, and presented a kriging-assisted stochastic process discretization method to obtain the time-variant reliability. On the basis of the concept of the composite limit state, Li et al. [18] presented a sampling-based method for high-dimensional time-variant reliability analysis by using the generalized subset simulation (GSS). Straub et al. [32] computed the interval failure probability by subset simulation, and then used FORM to evaluate the cumulative failure probability. Chakraborty and Tesfamariam [5] developed a subset simulation-based method for reliability problem with space-time variant. Regardless of the outcrossing rate based methods, extreme value based methods or composite limit state random methods, most of them are based on analytical approximation, surrogate models or sampling. It is still a thorny issue to balance the accuracy and efficiency for estimating the time-variant reliability.

In this work, an adaptive PC-Kriging method is developed for time-variant reliability analysis. It uses the PC-Kriging with better accuracy and efficiency [31] to model the instantaneous responses instead of the traditional Kriging. A new updating strategy combining the U- and H- learning functions is proposed to refine the PCK models

of instantaneous responses. One or two best samples are identified for updating the PCK models in each updating process until the new stopping criterion is satisfied.

This paper is organized as follows. The definition of time-variant reliability problem is provided in Section 2. Section 3 describes the proposed adaptive PC-Kriging method in detail. In Section 4, four examples are employed to illustrate the performance of the APCK method. Conclusions are drawn in Section 5.

## 2. Time-variant reliability problem

The performance of a structure is dynamic since the existence of time-variant uncertainties such as the loading condition characterized by stochastic process. Therefore, the probability that a structure performance satisfies the design requirement varies with time. In other words, reliability is a function of time. The time-variant reliability in a time period of interest  $[0, t_f]$  is defined as:

$$R(0, t_f) = \Pr \{G = g(X, Y(t), t) > 0, \forall t \in [0, t_f]\} \quad (1)$$

where  $\forall$  means “for all”.  $G$  is the structural response, and  $G > 0$  indicates the structure is in safe state; otherwise a failure occurs. Here,  $g(\bullet)$  represents the limit state function (LSF) of the structure,  $[X_1, X_2, \dots, X_n]$  is the input random vector with  $n$ -dimensions,  $Y(t) = [Y_1(t), Y_2(t), \dots, Y_m(t)]$  is the  $m$ -dimensional stochastic process vector, and  $t$  is time factor.

Correspondingly, the cumulative failure probability is given by:

$$P_f(0, t_f) = 1 - R(0, t_f) = \Pr \{G = g(X, Y(t), t) < 0, \exists t \in [0, t_f]\} \quad (2)$$

where  $\exists$  stands for “there exists at least one”. In this study, we calculated the cumulative failure probabilities with respect to time to complete the time-variant reliability analysis.

## 3. Proposed method

### 3.1. Overview

Four main modules are involved in the proposed APCK method which are designed to assess the time-variant reliability problem with random process. Discretization of stochastic process is the first module of the APCK method, which aims to compute the probabilistic characteristics of input stochastic process in a time-variant reliability analysis problem. This module makes it possible to obtain the time-dependent response for estimating the time-variant reliability. The next module is the construction of PCK models for the instantaneous responses of a LSF. Based on the constructed PCK models, the time-dependent responses can be predicted to obtain the failure samples for calculating the cumulative failure probabilities. In order to improve the efficiency of PCK models construction and reduce the error of time-variant reliability, the module of a new updating strategy is developed. In this module, the U- and H- learning functions are combined to search the best updating samples to refine the constructed PCK models, and a stopping criterion is used to determine whether the PCK models meet the given required tolerance. The last module employs MCS to calculate the cumulative failure probabilities based on the time-dependent responses predicted by the final PCK models. The modules of the APCK method as shown in Fig. 1.

One new contribution to the APCK method is to estimate the time-variant reliability by employing the PCK models to approximate the instantaneous responses directly instead of modeling the response extreme values. The high-precision of the PCK models of the instantaneous responses is easy to implement since the response itself is less nonlinear than its response extreme value. In addition, the repeated process of obtaining the response extreme values is avoided and then

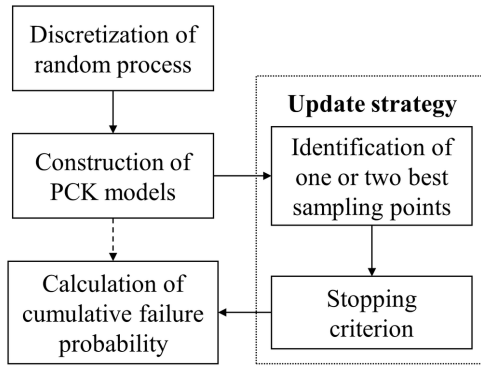


Fig. 1. Modules of the APCK method

the computational cost is reduced. A new update strategy is proposed to refine the PCK models in terms of the sign misjudgment probability and the uncertainty of model prediction. Both U- and H- learning functions are integrated to identify one or two best samples to improve the accuracy and updating efficiency of PCK models. Correspondingly, a new stopping criterion based on the combination of U- and H- learning criteria is also presented to terminate the updating process.

### 3.2. Discretization of stochastic process

Generally, the LSF of a time-variant reliability problem is a complex stochastic process due to the propagation of the input random variables  $\mathbf{X}$  and random processes  $\mathbf{Y}(t)$ . The samples of time-dependent random response of the LSF are the basis for assessing the cumulative failure probability in a time interval. Therefore, generating samples of random variables  $\mathbf{X}$  and realizations of stochastic process  $\mathbf{Y}(t)$  is the first step for time-variant reliability analysis. Discretization strategy is an effective way to deal with stochastic processes  $\mathbf{Y}(t)$ . The commonly used discretization methods mainly include the orthogonal series expansion (OSE) method [25], the Karhunen-Loève (KL) method [13] and the expansion optimal linear estimation (EOLE) method [17]. In this work, the EOLE is utilized to discrete the stochastic processes  $\mathbf{Y}(t)$ .

The EOLE method uses a set of random variables and time to represents a Gaussian process characterized by its mean function  $\mu_Y(t)$ , standard deviation function  $\sigma_Y(t)$  and autocorrelation function  $\rho_Y(t)$ . The time interval  $[0, t_f]$  is firstly discretized into  $s$  time instants  $t_i, i=1, 2, \dots, s$  with a step size  $\Delta t$ , and  $s = t_f / \Delta t + 1$ . Then the correlation matrix  $C$  of time instants  $t_i$  can be described as:

$$C = \begin{pmatrix} \rho_Y(t_1, t_1) & \rho_Y(t_1, t_2) & \cdots & \rho_Y(t_1, t_s) \\ \rho_Y(t_2, t_1) & \rho_Y(t_2, t_2) & \cdots & \rho_Y(t_2, t_s) \\ \vdots & \vdots & \ddots & \vdots \\ \rho_Y(t_s, t_1) & \rho_Y(t_s, t_2) & \cdots & \rho_Y(t_s, t_s) \end{pmatrix}_{s \times s} \quad (3)$$

After the Eigen decomposition of correlation matrix  $C$ , the stochastic processes  $\mathbf{Y}(t)$  is reconstructed by:

$$\mathbf{Y}(t) = \mu_Y(t) + \sigma_Y(t) \sum_{i=1}^l \frac{Z_i \xi_i^T}{\sqrt{\eta_i}} C_Y(t) \quad (4)$$

where  $\eta_i$  and  $\xi_i$  are the eigenvalues and eigenvectors of the correlation matrix  $C$ , respectively.  $Z_i$  are independent standard normal random variables.  $C_Y(t)$  is a time-dependent function vector whose components are  $\rho_Y(t, t_i), i=1, 2, \dots, s$ .  $l$  is the number of major eigenvalues of  $C$  used to construct the random process.

Once the random process is discretized, the LSF with both random variables and stochastic process is converted into one that only

involving random variables and explicit time parameter, which is described as:

$$g(\mathbf{X}, \mathbf{Y}(t), t) = g(\mathbf{X}, \mathbf{Z}, t) \quad (5)$$

Thus, the time-dependent responses can be calculated by generating the samples of random variables  $\mathbf{X}$  and  $\mathbf{Z}$  based on their probability distributions. Then, the cumulative failure probability can be rewritten as follow:

$$P_f(0, t_f) = \Pr \{ G = g(\mathbf{X}, \mathbf{Z}, t) < 0, t \in [0, t_f] \} \quad (6)$$

Although the discretization method tackle the issue of input random samples generation, the acquisition of responses as a stochastic process still cannot be directly realized. For this reason, the time-dependent response  $G$  within the time period  $[0, t_f]$  is represented by its instantaneous responses  $G_{t_i} = g(\mathbf{X}, \mathbf{Z}, t)$  at all time instant  $t_i (i=1, 2, \dots, s)$  in this work.

### 3.3. PC-Kriging model construction for instantaneous response

It is very time-consuming to perform direct MCS with the original LSF for evaluating the time-variant reliability. In order to reduce the computational cost, constructing a surrogate model for the original LSF is a popular and efficient strategy to predict the true instantaneous response  $G_{t_i}$ .

Kriging model is widely applied in reliability analysis due to its advantages of unbiased minimum variance estimation. A Kriging model includes two parts: a deterministic regression part and a random process, which are used to provide global and local approximation for the response of computational model, respectively. Let  $\mathbf{W}$  denotes the input random variables  $[\mathbf{X}, \mathbf{Z}]$  for simplification. The time-variant LSF for a given time instant  $t_i (i=1, 2, \dots, s)$  is only the function of input random variables  $\mathbf{W}$ , so it can be replaced by Kriging model as follows:

$$g_{t_i}(\mathbf{w}) = \mathbf{f}^T(\mathbf{w})\boldsymbol{\beta} + z(\mathbf{w}) \quad (7)$$

where  $\mathbf{f}(\mathbf{w}) = [f_1(\mathbf{w}), f_2(\mathbf{w}), \dots, f_b(\mathbf{w})]$ ; is the vector of basis function and  $b$  is the number of basis function.  $\boldsymbol{\beta} = [\beta_1, \beta_2, \dots, \beta_b]$  represents the  $b$ -dimensional basis function coefficient vector.  $z(\mathbf{w})$  is a stationary Gaussian process with zero mean. The covariance function of  $z(\mathbf{w})$  is:

$$\text{cov}(z(\mathbf{w}_i), z(\mathbf{w}_j)) = \sigma^2 R(\mathbf{w}_i, \mathbf{w}_j) \quad (8)$$

in which  $\sigma^2$  is the variance of  $z(\mathbf{w})$ ,  $R(\mathbf{w}_i, \mathbf{w}_j)$  is the correlation function between two samples  $\mathbf{w}_i$  and  $\mathbf{w}_j$ . Gaussian correlation function is the most widely used correlation function, and its formula is given by:

$$R(\mathbf{w}_i, \mathbf{w}_j) = \prod_{k=1}^n \exp \left\{ -\theta_k (w_i^k - w_j^k)^2 \right\} \quad (9)$$

where  $n$  is the number of variables in  $\mathbf{W}$ ,  $w_i^k$  is the  $k$ th component of  $\mathbf{w}_i$ ,  $\theta_k$  is the  $k$ th correlation parameters, respectively.

Obviously, the solutions of parameters  $\boldsymbol{\beta}$ ,  $\sigma^2$  and  $\theta_k$  are the basis for building a Kriging model. Given  $N$  samples  $\mathbf{W} = [\mathbf{w}_1, \mathbf{w}_2, \dots, \mathbf{w}_N]$  and their corresponding instantaneous responses  $\mathbf{G}_{t_i} = [G_{t_i}^1, G_{t_i}^2, \dots, G_{t_i}^N]$ , and the generalized least squares regres-

sion is employed, then the basis function coefficient vector and the variance of  $z(\mathbf{w})$  can be estimated respectively by:

$$\hat{\beta} = (F^T R^{-1} F)^T R^{-1} G_{t_i} \quad (10)$$

$$\hat{\sigma}^2 = \frac{1}{N} (G_{t_i} - F \hat{\beta})^T R^{-1} (G_{t_i} - F \hat{\beta}) \quad (11)$$

where  $F = [f_j(\mathbf{w}_i)]_{N \times b}$ ,  $R = [R(\mathbf{w}_i, \mathbf{w}_j)]_{N \times N}$  is the correlation matrix. However, the correlation parameters  $\theta_k$  in Eq. (10) and (11) are still to be determined, it can be obtained by the maximum likelihood estimation:

$$\theta = \arg \min_{\theta} \left\{ \frac{N}{2} \ln(\hat{\sigma}^2) + \frac{1}{2} \ln[\det(R)] \right\} \quad (12)$$

As a result, the prediction of instantaneous response at an arbitrary sample  $\mathbf{w}$  is given by:

$$\hat{g}_{t_i}^K(\mathbf{w}) = \mu_{\hat{g}_{t_i}^K}(\mathbf{w}) = f^T(\mathbf{w}) \hat{\beta} + r^T(\mathbf{w}) R^{-1} (G_{t_i} - F \hat{\beta}) \quad (13)$$

in which  $r(\mathbf{w}) = [R(\mathbf{w}, \mathbf{w}_1), R(\mathbf{w}, \mathbf{w}_2), \dots, R(\mathbf{w}, \mathbf{w}_N)]^T$  is the vector of correlation between the sample  $\mathbf{w}$  and all the given samples. The Kriging variance can be expressed as:

$$\hat{\sigma}_{\hat{g}_{t_i}^K}^2(\mathbf{w}) = \hat{\sigma}^2 \left[ 1 + u^T(\mathbf{w}) (F^T R^{-1} F)^{-1} u(\mathbf{w}) - r^T(\mathbf{w}) R^{-1} r(\mathbf{w}) \right] \quad (14)$$

where  $u(\mathbf{w}) = F^T R^{-1} r(\mathbf{w}) - f(\mathbf{w})$ .

PC-Kriging (PCK) is an improved meta-modeling technique which takes advantages of polynomial chaos expansion (PCE) and Kriging model. In PCK, PCE is utilized to replace the regression basis function part of the original Kriging to enhance the global approximation accuracy since its capability to capture the global behavior of computational model, and the local variability is still approximated by the Gaussian process of original Kriging [30].

In PCE theory, a random response  $G$  with  $n$ -dimensional input independent random variables  $\mathbf{w} = [w_1, w_2, \dots, w_n]$  can be approximated by an infinite series of polynomials:

$$G(\mathbf{w}) = \sum_{i=0}^{\infty} c_i \psi_i(\mathbf{w}) \quad (15)$$

in which  $c_i$  are the PCE coefficients.  $\psi_i(\mathbf{w})$  are multivariable PCE basis and it can be expressed as the tensor product of univariate polynomials:

$$\psi_i(\mathbf{w}) = \prod_j^n \Phi_{i_j}(w_j) \quad (16)$$

where  $\Phi_{i_j}(w_j)$  is the polynomial of degree  $i_j$  in the  $j$ th variable  $w_j$ , and it satisfies the following orthogonality:

$$\langle \Phi_{i_j}(w_j), \Phi_{i_k}(w_j) \rangle = \int \Phi_{i_j}(w_j) \Phi_{i_k}(w_j) f_{w_j}(w_j) dw_j = \begin{cases} 0, & j \neq k \\ 1, & j = k \end{cases} \quad (17)$$

Note that  $f_{w_i}(w)$  is the  $i$ th marginal probability density function of  $\mathbf{w}$ .

To make PCE feasible, the series in Eq. (15) can be truncated after  $p$  terms. The most commonly used strategy is to retain polynomials whose total degree not exceeding a given order  $p$ , which corresponds to a multi-indices set:

$$A = \left\{ i_j \in N^n, \sum_{j=1}^n i_j \leq p \right\} \quad (18)$$

The cardinality of the multi-indices set  $A$  is the number of polynomials retained in the truncation, it can be calculated by:

$$P = \frac{p+n}{p!n!} \quad (19)$$

Thus, the truncated PCE is given by:

$$G(\mathbf{w}) = \sum_{i=0}^{P-1} c_i \psi_i(\mathbf{w}) \quad (20)$$

Finally, the PCK prediction of instantaneous response can be built by replacing the regression part in Eq. (7) with Eq. (20):

$$\hat{g}_{t_i}^{PCK}(\mathbf{w}) = \sum_{i=0}^{P-1} c_i \psi_i(\mathbf{w}) + z(\mathbf{w}) \quad (21)$$

The set of polynomials in Eq. can be determined by the least angle regression selection (LARS), and then the PCK model is calibrated as a usual Kriging model for construction [15, 40].

### 3.4. A new updating strategy for PCK model of instantaneous response

In the case of small sample data, the accuracy of time-variant reliability analysis highly depends on the fidelity of the PCK models of the instantaneous responses. In view of the characteristic of PCK prediction obeying the normal distribution, a new adaptive update strategy based on the U-learning function [8] and H-learning function [22] is developed for improving the accuracy and efficiency of PCK model construction.

The U-learning function chooses a best sample to refine the model from the perspective of probabilistic theory. For the PCK model of instantaneous responses at any time instant  $t_i$  ( $i=1, 2, \dots, s$ ), the U-learning function is expressed as:

$$U_{t_i}(\mathbf{w}) = \left| \frac{\mu_{\hat{g}_{t_i}^{PCK}}(\mathbf{w})}{\sigma_{\hat{g}_{t_i}^{PCK}}(\mathbf{w})} \right| \quad (22)$$

where  $\mu_{\hat{g}_{t_i}^{PCK}}(\mathbf{w})$  and  $\sigma_{\hat{g}_{t_i}^{PCK}}(\mathbf{w})$  represent the mean value and standard deviation of instantaneous response PCK model  $\hat{g}_{t_i}^{PCK}(\mathbf{w})$  at the sample  $\mathbf{w}$ , respectively.  $U_{t_i}(\mathbf{w}) \geq 2$  means that the wrong-signed probability of sample  $\mathbf{w}$  is less than 0.0228. The accuracy of PCK model is considered to be accurate when all the samples in the sample pool meet this condition. Thus, the stopping criterion is given by:

$$\min_{\mathbf{w} \in \mathbf{D}} U_{t_i}(\mathbf{w}) \geq 2 \quad (23)$$



where  $\mathbf{D}$  is a sample pool. And then the best sample used to refine the PCK model is determined by:

$$\mathbf{w}_{t_i}^{Unew} = \arg \min_{\mathbf{w} \in \mathbf{D}} U_{t_i}(\mathbf{w}) \quad (24)$$

The H-learning function refines the model based on the information entropy theory. The H-learning function for PCK model of instantaneous responses is expressed as:

$$H_{t_i}(\mathbf{w}) = \left| -\int_{g^-(\mathbf{w})}^{g^+(\mathbf{w})} f_{\hat{g}_{t_i}^{PCK}(\mathbf{w})}(\mathbf{w}) \ln f_{\hat{g}_{t_i}^{PCK}(\mathbf{w})}(\mathbf{w}) d\hat{g}_{t_i}^{PCK}(\mathbf{w}) \right|$$

$$= \left| \ln \left( \sqrt{2\pi} \sigma_{\hat{g}_{t_i}^{PCK}(\mathbf{w})} + \frac{1}{2} \right) \Phi \left( \frac{2\sigma_{\hat{g}_{t_i}^{PCK}(\mathbf{w})} - \mu_{\hat{g}_{t_i}^{PCK}(\mathbf{w})}}{\sigma_{\hat{g}_{t_i}^{PCK}(\mathbf{w})}} \right) \right.$$

$$\left. - \ln \left( \sqrt{2\pi} \sigma_{\hat{g}_{t_i}^{PCK}(\mathbf{w})} + \frac{1}{2} \right) \Phi \left( \frac{-2\sigma_{\hat{g}_{t_i}^{PCK}(\mathbf{w})} - \mu_{\hat{g}_{t_i}^{PCK}(\mathbf{w})}}{\sigma_{\hat{g}_{t_i}^{PCK}(\mathbf{w})}} \right) \right|$$

$$= \left| -\frac{2\sigma_{\hat{g}_{t_i}^{PCK}(\mathbf{w})} - \mu_{\hat{g}_{t_i}^{PCK}(\mathbf{w})}}{2} \phi \left( \frac{2\sigma_{\hat{g}_{t_i}^{PCK}(\mathbf{w})} - \mu_{\hat{g}_{t_i}^{PCK}(\mathbf{w})}}{\sigma_{\hat{g}_{t_i}^{PCK}(\mathbf{w})}} \right) \right.$$

$$\left. - \frac{2\sigma_{\hat{g}_{t_i}^{PCK}(\mathbf{w})} + \mu_{\hat{g}_{t_i}^{PCK}(\mathbf{w})}}{2} \phi \left( \frac{-2\sigma_{\hat{g}_{t_i}^{PCK}(\mathbf{w})} - \mu_{\hat{g}_{t_i}^{PCK}(\mathbf{w})}}{\sigma_{\hat{g}_{t_i}^{PCK}(\mathbf{w})}} \right) \right| \quad (25)$$

where  $g^+(\mathbf{w}) = 2\sigma_{\hat{g}_{t_i}^{PCK}(\mathbf{w})}$  and  $g^-(\mathbf{w}) = -2\sigma_{\hat{g}_{t_i}^{PCK}(\mathbf{w})}$ .  $\Phi(\cdot)$  and  $\phi(\cdot)$  are the cumulative distribution function (CDF) and probability density function (PDF) of standard normal variable, respectively. The value of  $H_{t_i}(\mathbf{w})$  represents the information entropy of the sample  $\mathbf{w}$ , which can be used to measure the uncertainty degree of PCK model prediction for this sample. Therefore, the sample with maximum uncertainty is chosen as the best sample to update the PCK model:

$$\mathbf{w}_{t_i}^{Hnew} = \arg \max_{\mathbf{w} \in \mathbf{D}} H_{t_i}(\mathbf{w}) \quad (26)$$

Then, the stopping criterion of H-learning function is defined by:

$$\max_{\mathbf{w} \in \mathbf{D}} H_{t_i}(\mathbf{w}) \leq \varepsilon_H \quad (27)$$

in which  $\varepsilon_H$  is set to 0.3 in this work as suggested in [8].

In reliability analysis, the basis of samples selection that contributes to the improvement of the surrogate model is divided into two aspects: the probability of sign misjudgment and the uncertainty of model prediction. The U-learning function identifies the sample with the highest probability of sign misjudgment to update the surrogate model and the H-learning function selects the one with the maximum prediction uncertainty to refine the model. Therefore, the proposed update strategy integrates the U- and H- learning functions to improve the accuracy and updating efficiency of PCK model from both aspects of sign misjudgment and prediction uncertainty. The correctness of sign predicted by the PCK model of instantaneous response has big influence on the final result of time-variant reliability analysis, which results in the dominate position of the U-learning function in the proposed updating strategy. While the H-learning function is a complement to the U-learning function.

The first step is to determine whether the signs of samples in the sample pool  $\mathbf{D}$  are all correct based on Eq. (23). If the stopping criterion of U-learning function in Eq. is satisfied, it is considered that the sign predicted by PCK model  $\hat{g}_{t_i}^{PCK}(\mathbf{w})$  is accurate, and then the H-learning function is used to refine the PCK model  $\hat{g}_{t_i}^{PCK}(\mathbf{w})$ . In this case, if the convergence condition in Eq. is not satisfied, then the new sample  $\mathbf{w}_{t_i}^{new} = \mathbf{w}_{t_i}^{Hnew}$  and its corresponding true instantaneous responses  $G_{t_i}^{new} = G_{t_i}^{Hnew} = g(\mathbf{w}_{t_i}^{Hnew}, t_i)$  are added into the training sample set  $\mathbf{T}$  to update the PCK model  $\hat{g}_{t_i}^{PCK}(\mathbf{w})$ ; otherwise, the PCK model  $\hat{g}_{t_i}^{PCK}(\mathbf{w})$  is considered to be accurate enough to terminate the updating process.

When Eq. (23) is not satisfied, which indicates that the sign of prediction of PCK model  $\hat{g}_{t_i}^{PCK}(\mathbf{w})$  is not credible. At this point, both the U- and H- learning functions are employed to improve the PCK model  $\hat{g}_{t_i}^{PCK}(\mathbf{w})$ . For that, a new stopping criterion is developed as follows:

$$\max_{\mathbf{w} \in \mathbf{D}} K_{t_i}(\mathbf{w}) = \frac{H_{t_i}(\mathbf{w})}{U_{t_i}(\mathbf{w})} \leq \varepsilon_K \quad (28)$$

where  $\varepsilon_K$  is obtained according to the thresholds of the stopping criteria for the U- and H- learning criteria, and its value is 0.15. If Eq. (28) holds, the accuracy of PCK model  $\hat{g}_{t_i}^{PCK}(\mathbf{w})$  meets the requirement without a subsequently updating process. Conversely, the new samples  $\mathbf{w}_{t_i}^{new} = [\mathbf{w}_{t_i}^{Unew}; \mathbf{w}_{t_i}^{Hnew}]$  are chosen based on Eq. (24) and Eq. (26), respectively, and their corresponding true instantaneous responses  $G_{t_i}^{new} = [G_{t_i}^{Unew}; G_{t_i}^{Hnew}] = [g(\mathbf{w}_{t_i}^{Unew}, t_i); g(\mathbf{w}_{t_i}^{Hnew}, t_i)]$  are added into the initial training sample set  $\mathbf{T}$  to update the PCK model  $\hat{g}_{t_i}^{PCK}(\mathbf{w})$ . It is worth to point out that the new sample  $\mathbf{w}_{t_i}^{Hnew}$  at this moment is selected by the H-learning function in the sample pool  $\mathbf{D}_1$  where  $\mathbf{D}_1 = \{\mathbf{w} | U_{t_i}(\mathbf{w}) \geq 2, \mathbf{w} \in \mathbf{D}\}$ . The detailed update procedure is presented in section 3.4.

Let  $\hat{g}_{t_i}^{APCK}(\mathbf{w})$  denote the predicted instantaneous response by the final PCK model, then an indicator function is defined as:

$$I(\mathbf{w})_{[0, t_f]} = \begin{cases} 1, & \min_{0 \leq t_i \leq t_j} \hat{g}_{t_i}^{APCK}(\mathbf{w}) < 0 \\ 0, & \text{otherwise} \end{cases} \quad (29)$$

where  $I(\mathbf{w})_{[0, t_f]}$  is the indicator function in the time interval of interest  $[0, t_f]$ . Based on Eq. (29), the cumulative failure probability in the time interval  $[0, t_f]$  is estimated by MCS as follows:

$$P_f(0, t_f) = \frac{1}{N_{MCS}} \sum_{i=1}^{N_{MCS}} I(\mathbf{w}_i)_{[0, t_f]} \quad (30)$$

when  $t_f$  changes from 0 to  $t_f$ , one can obtain a cumulative failure probability curve with respect to time, which is much more meaningful than a point estimation for reliability discussion.

### 3.5. Implementation procedure

The implementation procedure of the APCK method for time-variant reliability analysis is shown in Fig. 2. The detailed steps are presented as follows:

1. Parameter setting. Set the time step size  $\Delta t$ , the highest order  $p$  of PCK model, the number of initial samples  $N$  for constructing the initial PCK model.

2. Discretization of stochastic process. Time interval is  $[0, t_f]$  firstly discretized into  $s = t_f / \Delta t + 1$  time nodes  $t_i, i = 1, 2, \dots, s$  with time step size  $\Delta t$ . Then, the stochastic process  $Y(t)$  is converted into a function of the standard normal variables  $\mathbf{Z}$  by EOLE method.
3. Generation of initial training sample set. Generate sample pool  $\mathbf{D}$ . Then, select  $N$  samples  $\mathbf{W}$  from  $\mathbf{D}$  and evaluate their corresponding performance function instantaneous responses  $\mathbf{G}_{t_i} = g(\mathbf{W}, t_i), i = 1, 2, \dots, s$ .  $\mathbf{W}$  and  $\mathbf{G}_{t_i}$  constitute the initial training sample set  $\mathbf{T} = [\mathbf{W}, \mathbf{G}_{t_i}]$ .
4. PCK model construction. Build the PCK models based on  $\mathbf{T}$  by using the MATLAB toolbox UQLAB [24]. The Gaussian correlation function is used here as mentioned in section 3.2.
5. Judgment of the correctness of samples signs. Check whether the prediction signs of samples in  $\mathbf{D}$  are all credible based on the stopping criterion of U-learning function expressed in Eq. (23). If Eq. (23) is satisfied, then go to step 6. Otherwise, the samples in  $\mathbf{D}$  that satisfy Eq. (23) are composed into the sample pool  $\mathbf{D}_1 = \{\mathbf{w} | U_{t_i}(\mathbf{w}) \geq 2, \mathbf{w} \in \mathbf{D}\}$ , then go to step 9.
6. Identification of the best sample by the H-learning criterion. Search the best sample  $\mathbf{w}_{t_i}^{new} = \mathbf{w}_{t_i}^{Hnew}$  in  $\mathbf{D}$  based on the H-learning criterion described in Eq. (26).
7. Stopping criterion of the H-learning function. Check whether the stopping criterion of H-learning function expressed in Eq. (27) is satisfied. If not, go to step 8, otherwise go to step 12.
8. Evaluation of the true instantaneous response at the best sample. Calculate the true instantaneous response of performance function  $G_{t_i}^{new} = g(\mathbf{w}_{t_i}^{new}, t_i)$  at sample  $\mathbf{w}_{t_i}^{new}$ . Add  $\mathbf{w}_{t_i}^{new}$  and  $G_{t_i}^{new}$  into the training set  $\mathbf{W}$  and  $\mathbf{G}_{t_i}$ , respectively, denoted as  $\mathbf{W} = [\mathbf{W}; \mathbf{w}_{t_i}^{new}]$  and  $\mathbf{G}_{t_i} = [\mathbf{G}_{t_i}; G_{t_i}^{new}]$ . Then, back to step 3.
9. Identification of the two best samples by the U- and H- learning criteria. Search the two best samples  $\mathbf{w}_{t_i}^{new} = [\mathbf{w}_{t_i}^{Unew}, \mathbf{w}_{t_i}^{Hnew}]$  based on the U- and H- learning criteria. It is note that  $\mathbf{w}_{t_i}^{Unew}$  is searched in  $\mathbf{D}$  and  $\mathbf{w}_{t_i}^{Hnew}$  is searched in  $\mathbf{D}_1$ .
10. The proposed stopping criterion. Check whether the proposed stopping criterion expressed in Eq. (28) is satisfied. If not, go to step 11, otherwise go to step 12.
11. Evaluation of the true instantaneous responses at the two best samples. Calculate the true instantaneous responses of performance function  $\mathbf{G}_{t_i}^{new} = [g(\mathbf{w}_{t_i}^{Unew}, t_i), g(\mathbf{w}_{t_i}^{Hnew}, t_i)]$  at samples  $\mathbf{w}_{t_i}^{Unew}$  and  $\mathbf{w}_{t_i}^{Hnew}$ . Add  $\mathbf{w}_{t_i}^{new}$  and  $\mathbf{G}_{t_i}^{new}$  into the in-

itial set  $\mathbf{W}$  and  $\mathbf{G}_{t_i}$ , respectively, denoted as  $\mathbf{W} = [\mathbf{W}; \mathbf{w}_{t_i}^{new}]$  and  $\mathbf{G}_{t_i} = [\mathbf{G}_{t_i}; \mathbf{G}_{t_i}^{new}]$ . Then, back to step 3.

12. Estimation of the cumulative failure probabilities. Perform MCS on the final PCK model to predict instantaneous responses and then the cumulative failure probability curve can be obtained by Eq. (30).

## 4. Illustrative examples

Four examples are used to demonstrate the performance of the APCK method in this section. MCS, PHI2 and independent EGO [11] are also employed to solve these examples for the comparison of APCK method. To make sure that the results from MCS has a small coefficient of variance,  $10^6$  samples were used in the first three illustrative examples.

### 4.1. A mathematical example

A mathematical example [35] is adopted to demonstrate the performance of the APCK method. The time-variant performance function is given by:

$$g(\mathbf{X}, Y(t), t) = X_1^2 X_2 - 5X_1(1 + Y(t))t + (X_2 + 1)t^2 - 20 \quad (31)$$

where  $\mathbf{X} = [X_1, X_2]$  are the input normal random variables,  $Y(t)$  is a Gaussian process with zero mean and unit variance,  $t \in [0, 1]$ . The detailed distribution information of input random parameters are listed in Table 1.

Table 1. Distribution information of the mathematical example

Variables	Distribution	Mean	Std	Autocorrelation function
$X_1$	Normal	3.5	0.25	N/A
$X_2$	Normal	3.5	0.25	N/A
$Y(t)$	Gaussian process	0	1	$\rho(t_1, t_2) = \exp(-(t_2 - t_1)^2)$

In this example,  $\Delta t$  was set to 0.05 and then the time interval  $[0, 1]$  was discretized into  $s = 21$  time instants. Thus, the 21 eigenvalues of the correlation matrix for stochastic process  $Y(t)$  were

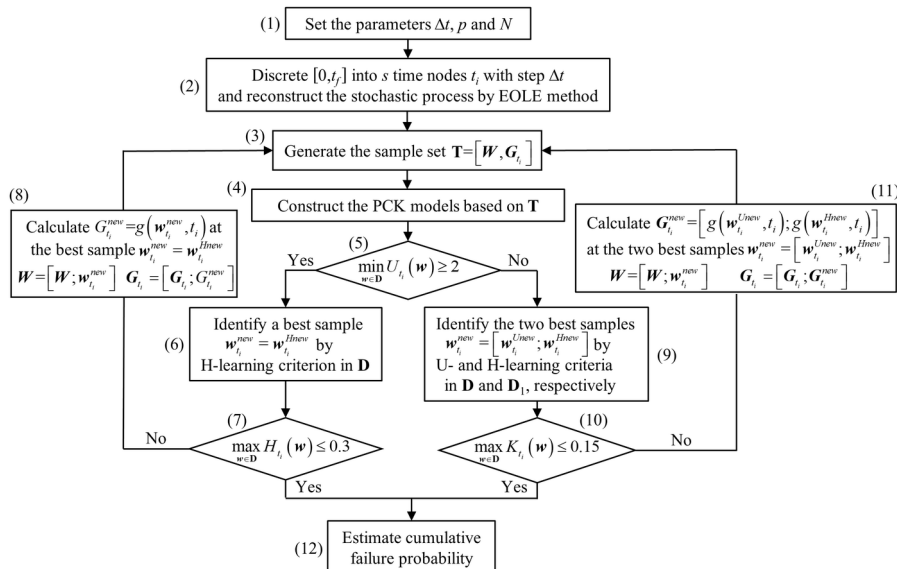


Fig. 2. Flowchart of the APCK method

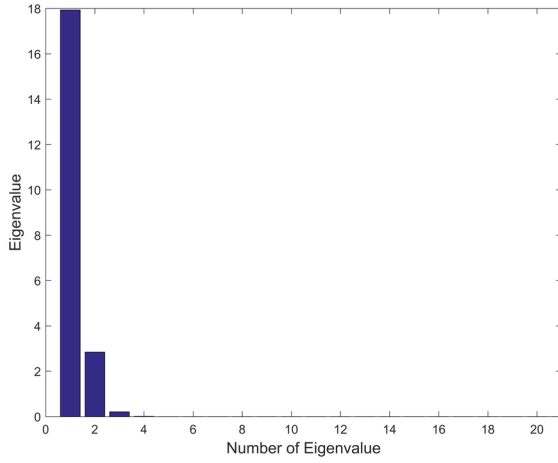


Fig. 3. Eigenvalues of  $Y(t)$

achieved, as shown in Fig. 3. It can be seen that the first two eigenvalues dominate the Gaussian process. As a result, two standard normal random variables  $\mathbf{Z} = [Z_1, Z_2]$  are utilized to represent  $Y(t)$ . Then, the input random variables of this mathematical example is  $\mathbf{W} = [X_1, X_2, Z_1, Z_2]$ .

MCS was employed as the benchmark approach in this work.  $10^6$  samples of  $\mathbf{W}$  were used by MCS to calculate the instantaneous responses of LSF at each time instants for obtaining the time-variant probabilities of failure. In the APCK method, the highest order  $p$  is set to 3 according to experience in the open literature and the initial PCK models for instantaneous responses at 21 time nodes were built by  $N = 25$  initial samples of  $\mathbf{W}$ . Then, the updating strategy proposed in section 3.3 were utilized to refine the 21 initial PCK models until the convergence condition is satisfied. After the 21 updated PCK models of instantaneous responses at 21 time instants were obtained, the time-variant probabilities of failure was estimated by performing MCS on Eq. (30).

Table 2. Time-variant probabilities of failure for the mathematical example

Time interval	MCS	APCK (Error %)	PHI2 (Error %)	Independent EGO (Error %)
[0, 0.2]	0.00132	0.00128 (3.03)	0.00120 (9.09)	0.00086 (34.85)
[0, 0.4]	0.03080	0.03104 (0.78)	0.02930 (4.87)	0.03034 (1.49)
[0, 0.6]	0.11910	0.119 (0.08)	0.11043 (7.28)	0.11880 (0.25)
[0, 0.8]	0.22052	0.22077 (0.11)	0.19620 (11.03)	0.22128 (0.34)
[0, 1.0]	0.29946	0.30012 (0.22)	0.25757 (13.99)	0.29871 (0.25)
NOF	$10^6$	25 + 36	640	7977

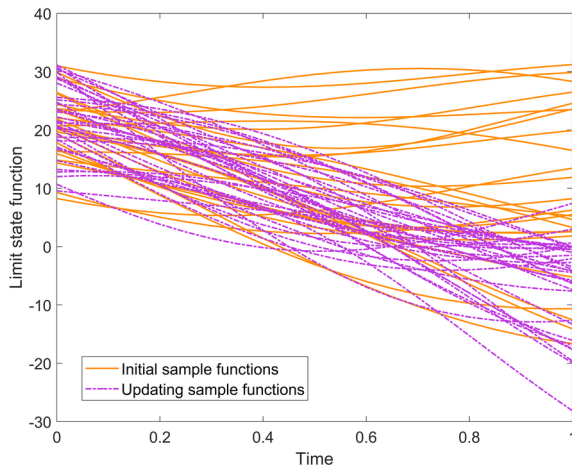


Fig. 4. Sample functions of the LSF used in the mathematical example

The results from direct MCS, APCK, PHI2 and independent EGO methods are presented in Table 2 and Fig. 5. It can be seen from the results that the time-variant probabilities of failure obtained by APCK is very close to those estimated by direct MCS within the whole time interval. The overall accuracy of PHI2 is low, while the independent EGO has a large error in the time period with small failure probability. The term of NOF in Table 2 represents the number of function evaluations. In Fig. 4, the orange solid lines are the 25 initial sample functions of the LSF response used in APCK to construct the initial PCK models and the purple dashed lines are the 36 updating sample functions for updating the PCK models. One sample function means that one function evaluation so that the total NOF of APCK is 61. In terms of efficiency, a total of 640 and 7977 function evaluations were needed by the PHI2 and independent EGO to achieve the results of time-variant probabilities of failure. Therefore, APCK can obtain an accurate results of time-variant reliability analysis with less computational cost.

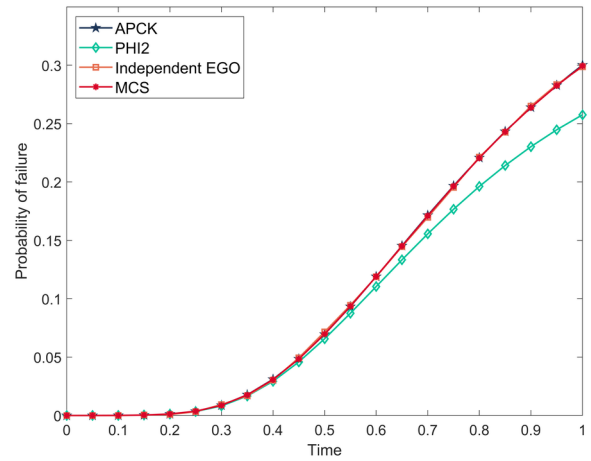


Fig. 5. Time-variant failure probability curves of the mathematical example

## 4.2. A corroded beam structure

In this section, the corrosion problem in a steel bending beam is used to demonstrate the performance of APCK. The corroded beam structure [20] is shown in Fig. 6, and it has a length of  $L = 5$  m and a rectangular cross section with width  $b_0$  and height  $h_0$ . The beam is uniformly loaded by its own weight, which is expressed as  $d = \rho_{st} b_0 h_0$  (N/m).  $\rho_{st} = 78.5$  kN/m<sup>3</sup> is the steel density. In addition, a dynamic concentrated load  $F(t)$  is also applied at the mid span simultaneously.

The corrosion phenomenon is a process which depends on time. Assuming that the stiffness has been lost in the corroded area of beam, the remained cross section with intact stiffness after a period of time  $t$  is given by:

$$S(t) = b(t)h(t) \quad (32)$$

where  $b(t) = b_0 - 2kt$  and  $h(t) = h_0 - 2kt$  is the parameter indicating the rate of corrosion. Then, the bending moment of beam at the midpoint is derived as:

$$M(t) = \frac{F(t)L}{4} + \frac{\rho_{st} b_0 h_0 L^2}{8} \quad (33)$$

The ultimate bending moment for the beam is given by:

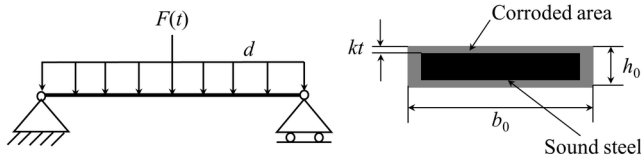


Fig. 6. A corroded beam structure

$$M_u(t) = \frac{b(t)h^2(t)}{4} f_y \quad (34)$$

As a result, the time-variant LSF of the beam is expressed as:

$$g(X, Y(t), t) = M_u(t) - M(t) = \frac{b(t)h^2(t)}{4} f_y - \left( \frac{F(t)L}{4} + \frac{\rho_{sr} b_0 h_0 L^2}{8} \right) \quad (35)$$

where  $f_y$  is the steel yield stress.  $f_y$ ,  $b_0$  and  $h_0$  are all random variables with lognormal distribution.  $F(t)$  is a Gaussian process and  $t \in [0, 20]$  years. The distribution parameters are gathered in Table 3.

Table 3. Distribution information of the corroded beam structure

Variables	Distribution	Mean	Std	Autocorrelation function
(MPa)	Lognormal	240	24	N/A
(m)	Lognormal	0.2	0.01	N/A
(m)	Lognormal	0.03	0.003	N/A
(N)	Gaussian process	3500	700	

The time interval  $[0, 20]$  was discretized into  $s = 21$  time instants with a step  $\Delta t = 1$  year. Then, the stochastic process loading  $F(t)$  was reconstructed by the first six maximum eigenvalue of its correlation matrix and six standard normal random variables  $Z = [Z_1, Z_2, \dots, Z_6]$ . Then, there are 9 input random parameters  $W = [f_y, b_0, h_0, Z_1, Z_2, \dots, Z_6]$  for the corroded beam example.

The reference result were provided by the direct MCS using  $10^6$  samples of  $W$ . The highest order  $p = 3$  was adopted for the PCK model generation in the APCK method.  $N = 80$  initial samples of  $W$  were used to build the initial PCK models of the instantaneous responses at 21 time nodes in sequence. Then, 95 updating samples were chosen to refine the 21 PCK models by using the developed updating strategy. The cumulative failure probabilities of the corroded beam over five sub-intervals are presented in Table 4. The time-variant probability of failure curves for direct MCS, APCK, PHI2 and independent EGO are shown in Fig. 7.

Table 4. Time-variant probabilities of failure for the corroded beam structure

Time interval	MCS	APCK (Error %)	PHI2 (Error %)	Independent EGO (Error %)
[0, 4]	0.01416	0.01388 (1.98)	0.04574 (223.02)	0.00687 (51.48)
[0, 8]	0.02137	0.02146 (0.42)	0.09029 (322.51)	0.01409 (34.07)
[0, 12]	0.02930	0.02923 (0.23)	0.14238 (385.94)	0.02346 (19.93)
[0, 16]	0.03787	0.03812 (0.66)	0.20214 (433.77)	0.03188 (15.82)
[0, 20]	0.04702	0.04735 (0.71)	0.26910 (472.31)	0.04202 (10.63)
NOF	$10^6$	80 + 95	1441	21044

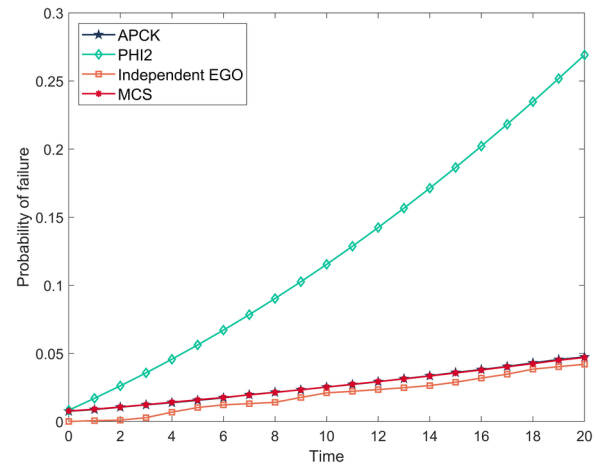


Fig. 7. Time-variant failure probability curves of the corroded beam structure

It can be observed from Table 4 that the computational results of PHI2 and independent EGO are very inaccurate, while the maximum error of APCK in the whole time interval is 1.98%. This shows the good performance of APCK in accuracy, and it also can be verified in Fig. 7. Compared with PHI2 and independent EGO, the proposed APCK has a good computational efficiency. 80 initial evaluations of LSF were employed to build the 21 initial PCK models and 95 evaluations for updating stage. In other words, the total computational cost of APCK is only 175 evaluations of LSF. This is about the 12% of the computational cost of PHI2 and much less than the 21044 evaluations of independent EGO. It demonstrates that APCK is efficient and accurate in solving the time-variant reliability problem.

#### 4.3. Hydrokinetic turbine blade

Hydrokinetic turbine is a mechanism that realizes the conversion of the kinetic energy of water through its blades rotation driven by flowing water. The time-variant reliability analysis of its blade is used to demonstrate the performance of the APCK method. The cross section of a hydrokinetic turbine blade [35] determined by three geometry parameters  $d_1$ ,  $d_2$  and  $d_3$  are shown in Fig. 8. The monthly velocity of river loaded on the blade is characterized by a stochastic process  $v(t)$  with mean  $\mu_v(t)$ , standard deviation  $\sigma_v(t)$  and autocorrelation function  $\rho_v(t_1, t_2)$ .  $\mu_v(t)$ ,  $\sigma_v(t)$  and  $\rho_v(t_1, t_2)$  are given by:

$$\mu_v(t) = \sum_{i=1}^4 a_i^m \sin(b_i^m t + c_i^m) \quad (36)$$

$$\sigma_v(t) = \sum_{j=1}^4 a_j^s \exp\left\{-\left[(t - b_j^s)c_j^s\right]^2\right\} \quad (37)$$

$$\rho_v(t_1, t_2) = \cos(2\pi(t_2 - t_1)) \quad (38)$$

where the constant parameters  $a$ ,  $b$  and  $c$  can be found in [35]. Then, the bending moment at the root of blade is calculated by:

$$M_b = \frac{1}{2} \rho v^2(t) C_m \quad (39)$$

Note that  $\rho = 10^3 \text{ kg/m}^3$  is the water density, and  $C_m = 0.3422$  is the coefficient of moment. Thus, the LSF of hydrokinetic turbine blade is defined by:



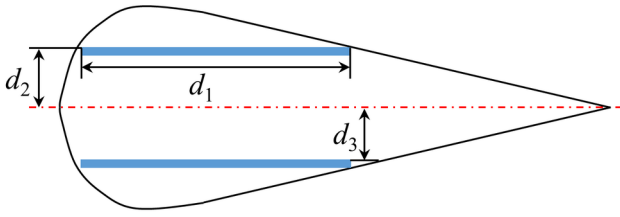


Fig. 8. Cross section of the turbine blade

$$g(X, Y(t), t) = \varepsilon_{allow} - \frac{d_2 M_b}{EI_a} \quad (40)$$

where  $\varepsilon_{allow}$  is the allowable strain of the material.  $E = 14 \text{ GPa}$  is the Young's modulus, and  $I_a$  is the moment of inertia at the root of the blade, which is expressed as:

$$I_a = \frac{2}{3} d_1 (d_2^3 - d_3^3) \quad (41)$$

The detailed statistical information of the inputs are listed in Table 5.

Table 5. Distribution information of the hydrokinetic turbine blade

Variables	Distribution	Mean	Std	Autocorrelation function
(m)	Normal	0.22	$2.2 \times 10^{-3}$	N/A
(m)	Normal	0.025	$2.5 \times 10^{-4}$	N/A
(m)	Normal	0.019	$1.9 \times 10^{-4}$	N/A
(m)	Normal	0.025	$2.5 \times 10^{-4}$	N/A
(m/s)	Gaussian process			

A time step  $\Delta t = 0.2$  month was used to discretize the time interval  $[0, 12]$  months into  $s = 61$  time instants. Then, the eigen analysis was performed on the correlation matrix of the random process  $v(t)$  for obtaining the eigenvalues and eigenvectors. Finally, two largest eigenvalues and two standard normal random variables  $\mathbf{Z} = [Z_1, Z_2]$  are utilized to represent the stochastic process  $v(t)$ . Let  $\mathbf{W} = [d_1, d_2, d_3, \varepsilon_{allow}, Z_1, Z_2]$  denotes the random inputs of the hydrokinetic turbine blade, and then the dimension of turbine blade problem is 6.

The direct MCS was performed on the LSF of the hydrokinetic turbine blade with  $10^6$  samples for achieving the time-variant probability of failure. Fig. 9 shows ten realizations of the LSF, which indicates that the LSF is highly nonlinear.  $p$  is set to 2 in the APCK method, and then the 61 initial PCK models of instantaneous responses were constructed by  $N = 50$  initial samples of  $\mathbf{W}$ . The results are provided in Table 6 and Fig. 10, and the values in brackets of Table 6 are errors.

Table 6 and Fig. 10 show that the APCK method can achieve sufficient accuracy over the whole time interval with low computational cost. Both PHI2 and independent EGO methods have large computational errors, and the PHI2 method is much more efficient than the independent EGO method within the entire time period. It can be observed that the independent EGO method loses the local trend

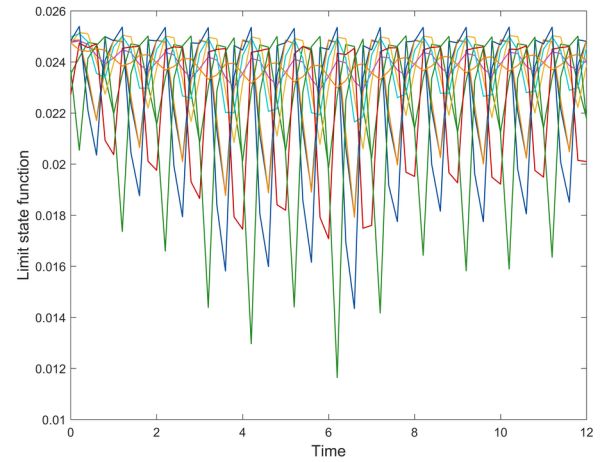


Fig. 9. Ten realizations of LSF for the turbine blade

characteristic of the cumulative failure probability curve, and its calculation results are all 0 in the time period  $[0, 6]$ . This indicates that the accuracy of independent EGO method is significantly limited in the case of LSF with strong nonlinearity. In comparison, the errors of APCK are all acceptable and the minimum error is 1.29%. In the same time period, the errors of APCK are all less than those of PHI2 and independent EGO methods. In addition, APCK is much more efficient than the PHI2 and independent EGO methods. A total of 145 function evaluations were required for APCK, it is far less than 3398 function evaluations used in the PHI2 method and 282015 function evaluations used in the independent EGO method. It is noted that the computational cost of the updating state is only 95 function evaluations in case of the strong nonlinearity of this example. This illustrates the high efficiency of the learning strategy of the proposed method.

#### 4.4. Turbo engine

The turbo engine is a kind of powerplant with extremely complex structure, which is widely used in various flight vehicles. A failure of turbo engine may lead to a catastrophic event. In this application, the

Table 6. Time-variant probabilities of failure for the hydrokinetic turbine blade

Time interval	MCS ( $10^{-4}$ )	APCK ( $10^{-4}$ )	PHI2 ( $10^{-4}$ )	Independent EGO ( $10^{-4}$ )
[0, 2]	0.10	0.07 (30.00%)	0.07 (30.00%)	0 (100%)
[0, 3]	0.40	0.37 (7.50%)	0.48 (20.00%)	0 (100%)
[0, 4]	5.00	5.16 (3.20%)	5.24 (4.80%)	0 (100%)
[0, 5]	6.40	6.57 (2.66%)	9.46 (47.81%)	0 (100%)
[0, 6]	6.70	7.05 (5.22%)	13.83 (106.42%)	0 (100%)
[0, 7]	16.30	16.09 (1.29%)	29.15 (78.83%)	22.76 (39.63%)
[0, 8]	16.30	16.09 (1.29%)	29.95 (83.74%)	22.76 (39.63%)
NOF	$10^6$	50 + 95	3398	282015

proposed APCK method is employed for the time-variant reliability analysis of a turbo engine.

As shown in Fig. 11, the turbo engine is mainly composed of turbo fan, turbo compressor, turbo disk and casing. The support stiffness ( $K_1, K_2$ ) and support damping ( $C_1, C_2$ ) are considered as random variables and obey normal distribution. A time-variant loading  $F(t)$  described as stochastic process is acted on the turbo fan shaft, which will lead to the displacement of the turbo fan. In this case, it is assumed the displacement of the turbo fan is greater than the allowable gap as a failure event. The implicit limit state function of turbo engine is described as follow:

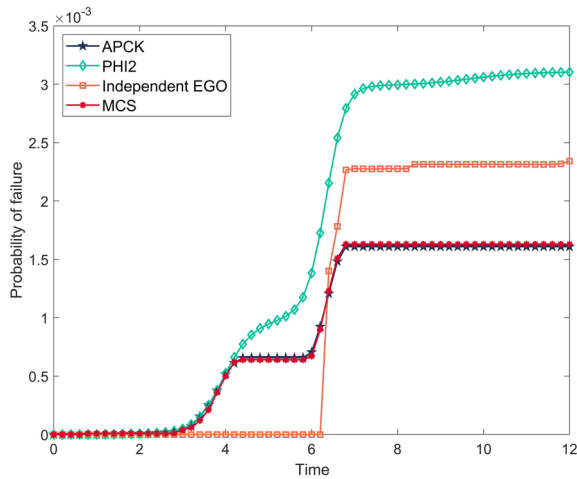


Fig. 10. Time-variant failure probability curves of the hydrokinetic turbine blade

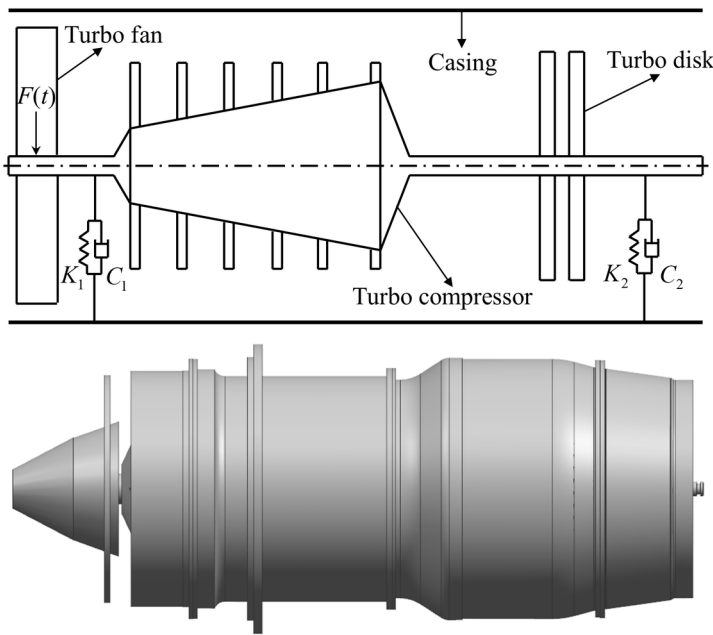


Fig. 11. Simplified model of a turbo engine

$$g(X, Y(t), t) = \delta_{allow} - \delta(K_1, K_2, C_1, C_2, F(t)) \quad (42)$$

where  $\delta_{allow} = 0.9\text{mm}$  is the allowable gap between the turbo fan and casing.  $\delta(\bullet)$  is the turbo fan displacement which can be obtained by the finite element method (FEM). All the parameters information are summarized in Table 7.

Table 7. Distribution information of the turbo engine

Variables	Distribution	Mean	Std	Autocorrelation function
$K_1$ (N/m)	Normal	$3.28 \times 10^7$	$3.28 \times 10^6$	N/A
$K_2$ (N/m)	Normal	$1.08 \times 10^7$	$1.08 \times 10^6$	N/A
$C_1$ (N·s/m)	Normal	1000	100	N/A
$C_2$ (N·s/m)	Normal	1000	100	N/A
$F(t)$ (N)	Gaussian process	10000	1000	$\rho(t_1, t_2) = \exp\left(-((t_2 - t_1)/0.5)^2\right)$

The FE model of turbo engine is presented in Fig. 12, in which 6800 nodes and 7426 elements are employed in this FE model. The stochastic loading  $F(t)$  is represented by 4 standard normally distributed variables  $Z = [Z_1, Z_2, Z_3, Z_4]$ , and the random inputs of turbo engine FE model are  $W = [K_1, K_2, C_1, C_2, Z_1, Z_2, Z_3, Z_4]$ . The turbo engine FE model is solved in  $[0, 1]$  hour with a time step  $\Delta t = 0.05$  hour for a dynamic analysis.

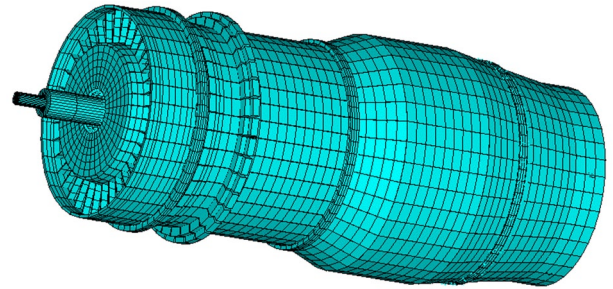


Fig. 12. The FE model for the turbo engine

In this example,  $N = 70$  runs of FE model of the turbo engine were used to obtain the displacement samples of the turbo fan for constructing the 21 initial PCK models at 21 time nodes. The 21 initial PCK models of the turbo fan displacement were refined by the 15 FE updating computations. The time-variant reliability results of the turbo engine obtained by APCK method is presented in Table 8 and Fig. 13.

Table 8. Time-variant probabilities of failure for the turbo engine

Time	APCK ( $10^{-3}$ )	Time	APCK ( $10^{-3}$ )
0	3.01	0.55	4.71
0.05	3.29	0.6	4.71
0.1	3.50	0.65	4.72
0.15	3.51	0.7	4.72
0.2	4.00	0.75	4.98
0.25	4.00	0.8	4.98
0.3	4.56	0.85	5.06
0.35	4.56	0.9	5.06
0.4	4.71	0.95	5.07
0.45	4.71	1	5.07
0.5	4.71	NOF	70 + 15

It can be seen from Fig. 13 that the failure probability of turbo engine increases rapidly from  $3.01 \times 10^{-3}$  to  $4.71 \times 10^{-3}$  over the time period  $[0, 0.4]$  hour, then gently reaches the peak value  $5.07 \times 10^{-3}$  for the remaining 0.6 hour. The final failure probability at the ending time is 1.68 times of the initial failure probability, which indicates that the time-variant reliability analysis is critical significant for the safety

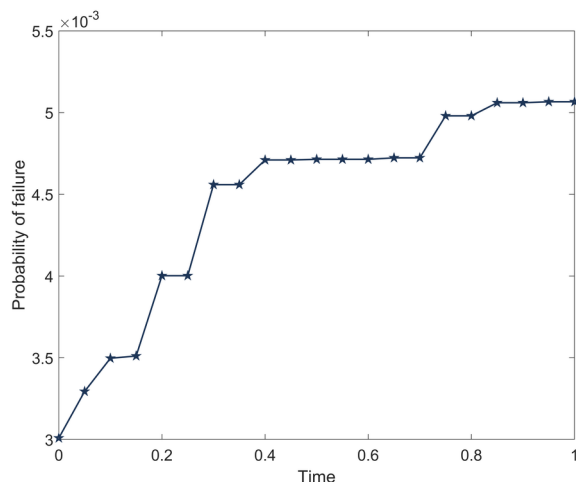


Fig. 13. Time-variant failure probability curves of the turbo engine

of turbo engine. In terms of computational efficiency, a total of 85 FE computations were needed by the proposed APCK. If the direct MCS are used to calculate the time-variant reliability for the implicit problems with FE model, the computational cost would be unacceptable.

## 5. Conclusions

This work presents an adaptive PC-Kriging method (APCK) that provides an estimation of cumulative failure probability curve for time-variant structural reliability analysis. The basic idea is to employ multiple PCK models to reconstruct the structural responses at

different time instants with an adaptive updating strategy. EOLE is employed to represent the input random process with a set of functions of random variables and time. Then, the PCK models at each time instants are constructed with a few initial samples and their corresponding instantaneous responses. In order to make the updating process adaptively, the characteristics of U- and H- learning functions are integrated to compose a new update strategy for the refinement of PCK models. PCK models are updated by one or two best samples in each updating stage to improve the accuracy and efficiency. In this update strategy, a new stopping criterion for the two best samples update is also presented. The time-variant failure probabilities can be achieved by performing MCS based on the final APCK models. The accuracy and efficiency of APCK are demonstrated by four examples. It can be seen from the results that the errors of APCK are acceptable in the whole time interval, which indicates that its accuracy is stable. In addition, the accuracy of APCK can be maintained even in the cases of strong nonlinearity and small probability of failure. In terms of efficiency, the number of function evaluations for APCK is close to the PHI2 and far less than the independent EGO. This shows that the computational cost can be greatly reduced by the APCK method. Furthermore, the APCK method is also efficient in solving the time-variant reliability problem with implicit limit state function. In future work, the APCK method will be extended to reliability-based design optimization and robust design optimization.

## Acknowledgement

*This work was supported by the Project Funded by the Priority Academic Program Development of Jiangsu Higher Education Institutions.*

## References

- Andrieu-Renaud C, Sudret B, Lemaire M. The PHI2 method: a way to compute time-variant reliability. *Reliability Engineering & System Safety* 2004; 84(1): 75–86, <https://doi.org/10.1016/j.res.2003.10.005>.
- Breitung K. Asymptotic approximations for probability integrals. *Probabilistic Engineering Mechanics* 1989; 4(4): 187–190, [https://doi.org/10.1016/0266-8920\(89\)90024-6](https://doi.org/10.1016/0266-8920(89)90024-6).
- Breitung K. Asymptotic crossing rates for stationary Gaussian vector processes. *Stochastic Processes and their Applications* 1988; 29(2): 195–207, [https://doi.org/10.1016/0304-4149\(88\)90037-3](https://doi.org/10.1016/0304-4149(88)90037-3).
- Cai C-H, Lu Z-H, Leng Y et al. Time-Dependent Structural Reliability Assessment for Nonstationary Non-Gaussian Performance Functions. *Journal of Engineering Mechanics* 2021; 147(2): 04020145, [https://doi.org/10.1061/\(ASCE\)EM.1943-7889.0001883](https://doi.org/10.1061/(ASCE)EM.1943-7889.0001883).
- Chakraborty S, Tesfamariam S. Subset simulation based approach for space-time-dependent system reliability analysis of corroding pipelines. *Structural Safety* 2021; 90: 102073, <https://doi.org/10.1016/j.strusafe.2020.102073>.
- Chen J-B, Li J. The extreme value distribution and dynamic reliability analysis of nonlinear structures with uncertain parameters. *Structural Safety* 2007; 29(2): 77–93, <https://doi.org/10.1016/j.strusafe.2006.02.002>.
- Ebrahimian M, Pirouzmmand A, Rabiee A. Developing a method for time-variant reliability assessment of passive heat removal systems in nuclear power plants. *Annals of Nuclear Energy* 2021; 160: 108365, <https://doi.org/10.1016/j.anucene.2021.108365>.
- Echard B, Gayton N, Lemaire M. AK-MCS: An active learning reliability method combining Kriging and Monte Carlo Simulation. *Structural Safety* 2011; 33(2): 145–154, <https://doi.org/10.1016/j.strusafe.2011.01.002>.
- Hu Y, Lu Z, Wei N, Zhou C. A single-loop Kriging surrogate model method by considering the first failure instant for time-dependent reliability analysis and safety lifetime analysis. *Mechanical Systems and Signal Processing* 2020; 145: 106963, <https://doi.org/10.1016/j.ymssp.2020.106963>.
- Hu Z, Du X. A Sampling Approach to Extreme Value Distribution for Time-Dependent Reliability Analysis. *Journal of Mechanical Design* 2013; 135(7): 071003, <https://doi.org/10.1115/1.4023925>.
- Hu Z, Du X. Mixed Efficient Global Optimization for Time-Dependent Reliability Analysis. *Journal of Mechanical Design* 2015; 137(5): 051401, <https://doi.org/10.1115/1.4029520>.
- Hu Z, Mahadevan S. A Single-Loop Kriging Surrogate Modeling for Time-Dependent Reliability Analysis. *Journal of Mechanical Design* 2016; 138(6): 061406, <https://doi.org/10.1115/1.4033428>.
- Huang S P, Quek S T, Phoon K K. Convergence study of the truncated Karhunen–Loeve expansion for simulation of stochastic processes. *International Journal for Numerical Methods in Engineering* 2001; 52(9): 1029–1043, <https://doi.org/10.1002/nme.255>.
- Kanjilal O, Manohar C S. Time variant reliability estimation of randomly excited uncertain dynamical systems by combined Markov chain splitting and Girsanov's transformation. *Archive of Applied Mechanics* 2020; 90(11): 2363–2377, <https://doi.org/10.1007/s00419-020-01726-y>.
- Kersaudy P, Sudret B, Varsier N et al. A new surrogate modeling technique combining Kriging and polynomial chaos expansions – Application to uncertainty analysis in computational dosimetry. *Journal of Computational Physics* 2015; 286: 103–117, <https://doi.org/10.1016/j.jcp.2015.01.034>.

16. Lelièvre N, Beaurepaire P, Mattrand C, Gayton N. AK-MCsi: A Kriging-based method to deal with small failure probabilities and time-consuming models. *Structural Safety* 2018; 73: 1–11, <https://doi.org/10.1016/j.strusafe.2018.01.002>.
17. Li C, Der Kiureghian A. Optimal Discretization of Random Fields. *Journal of Engineering Mechanics* 1993; 119(6): 1136–1154, [https://doi.org/10.1061/\(ASCE\)0733-9399\(1993\)119:6\(1136\)](https://doi.org/10.1061/(ASCE)0733-9399(1993)119:6(1136)).
18. Li H-S, Wang T, Yuan J-Y, Zhang H. A sampling-based method for high-dimensional time-variant reliability analysis. *Mechanical Systems and Signal Processing* 2019; 126: 505–520, <https://doi.org/10.1016/j.ymssp.2019.02.050>.
19. Li J, Chen J, Chen Z. Developing an improved composite limit state method for time-dependent reliability analysis. *Quality Engineering* 2020; 32(3): 298–311, <https://doi.org/10.1080/08982112.2020.1735004>.
20. Li J, Chen J, Wei J et al. Developing an Instantaneous Response Surface Method t-IRS for Time-Dependent Reliability Analysis. *Acta Mechanica Sinica* 2019; 32(4): 446–462, <https://doi.org/10.1007/s10338-019-00096-5>.
21. Linxiong H, Huacong L, Kai P, Hongliang X. A novel kriging based active learning method for structural reliability analysis. *Journal of Mechanical Science and Technology* 2020; 34(4): 1545–1556, <https://doi.org/10.1007/s12206-020-0317-y>.
22. Lv Z, Lu Z, Wang P. A new learning function for Kriging and its applications to solve reliability problems in engineering. *Computers & Mathematics with Applications* 2015; 70(5): 1182–1197, <https://doi.org/10.1016/j.camwa.2015.07.004>.
23. Majcher M, Mourelatos Z, Tsianika V. Time-Dependent Reliability Analysis Using a Modified Composite Limit State Approach. *SAE International Journal of Commercial Vehicles* 2017; 10(1): 66–72, <https://doi.org/10.4271/2017-01-0206>.
24. Marelli S, Sudret B. UQLab: A Framework for Uncertainty Quantification in Matlab. *Vulnerability, Uncertainty, and Risk*, Liverpool, UK, American Society of Civil Engineers: 2014: 2554–2563, <https://doi.org/10.1061/9780784413609.257>.
25. Ping M H, Han X, Jiang C, Xiao X Y. A time-variant extreme-value event evolution method for time-variant reliability analysis. *Mechanical Systems and Signal Processing* 2019; 130: 333–348, <https://doi.org/10.1016/j.ymssp.2019.05.009>.
26. Qian H-M, Huang H-Z, Li Y-F. A novel single-loop procedure for time-variant reliability analysis based on Kriging model. *Applied Mathematical Modelling* 2019; 75: 735–748, <https://doi.org/10.1016/j.apm.2019.07.006>.
27. Qian H-M, Huang T, Huang H-Z. A single-loop strategy for time-variant system reliability analysis under multiple failure modes. *Mechanical Systems and Signal Processing* 2021; 148: 107159, <https://doi.org/10.1016/j.ymssp.2020.107159>.
28. Quezada del Villar A V, Rodríguez-Picón L A, JC Pérez-Olgún I, Méndez-González L C. Stochastic modelling of the temperature increase in metal stampings with multiple stress variables and random effects for reliability assessment. *Eksplotacja i Niezawodność - Maintenance and Reliability* 2019; 21(4): 654–661, <https://doi.org/10.17531/ein.2019.4.15>.
29. Rice S O. Mathematical Analysis of Random Noise. *Bell System Technical Journal* 1945; 24(1): 46–156, <https://doi.org/10.1002/j.1538-7305.1945.tb00453.x>.
30. Schöbi R, Sudret B, Marelli S. Rare Event Estimation Using Polynomial-Chaos Kriging. *ASCE-ASME Journal of Risk and Uncertainty in Engineering Systems, Part A: Civil Engineering* 2017; 3(2): D4016002, <https://doi.org/10.1061/AJRUA6.0000870>.
31. Schöbi R, Sudret B, Wirt J. Polynomial-chaos-based Kriging. *International Journal for Uncertainty Quantification* 2015; 5(2): 171–193, <https://doi.org/10.1615/Int.J.UncertaintyQuantification.2015012467>.
32. Straub D, Schneider R, Bismut E, Kim H-J. Reliability analysis of deteriorating structural systems. *Structural Safety* 2020; 82: 101877, <https://doi.org/10.1016/j.strusafe.2019.101877>.
33. Sudret B. Analytical derivation of the outcrossing rate in time-variant reliability problems. *Structure and Infrastructure Engineering* 2008; 4(5): 353–362, <https://doi.org/10.1080/15732470701270058>.
34. Wang W, Wang J, Fu J, Lu G. A moment-matching based method for the analysis of manipulator's repeatability of positioning with arbitrarily distributed joint clearances. *Eksplotacja i Niezawodność - Maintenance and Reliability* 2018; 21(1): 10–20, <https://doi.org/10.17531/ein.2019.1.2>.
35. Wang Z, Chen W. Confidence-based adaptive extreme response surface for time-variant reliability analysis under random excitation. *Structural Safety* 2017; 64: 76–86, <https://doi.org/10.1016/j.strusafe.2016.10.001>.
36. Wang Z, Wang P. A new approach for reliability analysis with time-variant performance characteristics. *Reliability Engineering & System Safety* 2013; 115: 70–81, <https://doi.org/10.1016/j.ress.2013.02.017>.
37. Xu J. A new method for reliability assessment of structural dynamic systems with random parameters. *Structural Safety* 2016; 60: 130–143, <https://doi.org/10.1016/j.strusafe.2016.02.005>.
38. Yang M, Zhang D, Han X. New efficient and robust method for structural reliability analysis and its application in reliability-based design optimization. *Computer Methods in Applied Mechanics and Engineering* 2020; 366: 113018, <https://doi.org/10.1016/j.cma.2020.113018>.
39. Yang M, Zhang D, Wang F, Han X. Efficient local adaptive Kriging approximation method with single-loop strategy for reliability-based design optimization. *Computer Methods in Applied Mechanics and Engineering* 2022; 390: 114462, <https://doi.org/10.1016/j.cma.2021.114462>.
40. Yu Z, Sun Z, Cao R et al. RCA-PCK: A new structural reliability analysis method based on PC-Kriging and radial centralized adaptive sampling strategy. *Proceedings of the Institution of Mechanical Engineers, Part C: Journal of Mechanical Engineering Science* 2021; 235(17): 3424–3438, <https://doi.org/10.1177/0954406220957711>.
41. Zhang D, Han X, Jiang C et al. Time-Dependent Reliability Analysis Through Response Surface Method. *Journal of Mechanical Design* 2017; 139(4): 041404, <https://doi.org/10.1115/1.4035860>.
42. Zhang D, Zhou P, Jiang C et al. A stochastic process discretization method combining active learning Kriging model for efficient time-variant reliability analysis. *Computer Methods in Applied Mechanics and Engineering* 2021; 384: 113990, <https://doi.org/10.1016/j.cma.2021.113990>.
43. Zhang X-Y, Lu Z-H, Zhao Y-G, Li C-Q. The GLO method: An efficient algorithm for time-dependent reliability analysis based on outcrossing rate. *Structural Safety* 2022; 97: 102204, <https://doi.org/10.1016/j.strusafe.2022.102204>.